

Recurrent infomax generates cell assemblies, avalanches, and simple cell-like selectivity

Takuma Tanaka¹, Takeshi Kaneko^{1,2} & Toshio Aoyagi^{2,3}

¹*Department of Morphological Brain Science, Graduate School of Medicine, Kyoto University, Japan*

²*CREST, JST*

³*Department of Applied Analysis and Complex Dynamical Systems, Graduate School of Informatics, Kyoto University, Japan*

Through evolution, animals have acquired central nervous systems (CNSs), which are extremely efficient information processing devices that improve an animal’s adaptability to various environments. It has been proposed that the process of information maximization (infomax¹), which maximizes the information transmission from the input to the output of a feedforward network, may provide an explanation of the stimulus selectivity of neurons in CNSs²⁻⁷. However, CNSs contain not only feedforward but also recurrent synaptic connections, and little is known about information retention over time in such recurrent networks. Here, we propose a learning algorithm based on infomax in a recurrent network, which we call “recurrent infomax” (RI). RI maximizes information retention and thereby minimizes information loss in a network. We find that feeding in external inputs consisting of information obtained from photographs of natural scenes into an RI-based model of a recurrent network results in the appearance of Gabor-like selectivity quite similar to that existing in simple cells

of the primary visual cortex (V1). More importantly, we find that without external input, this network exhibits cell assembly-like and synfire chain-like spontaneous activity⁸⁻¹⁰ and a critical neuronal avalanche¹¹⁻¹³. RI provides a simple framework to explain a wide range of phenomena observed in *in vivo* and *in vitro* neuronal networks, and it should provide a novel understanding of experimental results for multineuronal activity and plasticity from an information-theoretic point of view.

Recent advances in multineuronal recording have allowed us to observe phenomena in the recurrent networks of CNSs that are much more complex than previously thought to exist. The existence of interesting type of neuronal activity, such as patterned firing, synchronization, oscillation, and global state transitions has been revealed by multielectrode recording and calcium imaging¹⁴⁻¹⁸. However, in contrast to the rapidly accumulating experimental data, theoretical works attempting to account for this wide range of data are developing more slowly. To understand the behaviour exhibited by recurrent neuronal networks of CNSs, we investigated a network employing an RI algorithm that maximizes information retention. The role of RI is to allow a recurrent network to optimize the synaptic connection weight in order to maximize information retention and thereby minimize information loss by maximizing the mutual information of the temporally successive states of the network.

Here we briefly describe our recurrent network model, leaving the details to the Supplementary Notes. In this model, neurons were connected according to the weight matrix W_{ij} , and their firing states [$x_i(t) = 1$ (fire) and 0 (not fire)] at time step t are synchronously updated to time step

$t + 1$. The firing state $x_i(t + 1)$ of neuron i at time step $t + 1$ is determined stochastically with the firing probability

$$p_i(t + 1) = \frac{p_{\max}}{1 + \exp\left(-\sum_j W_{ij}(x_j(t) - \bar{p}_j) + h_i(t)\right)}, \quad (1)$$

where $h_i(t)$ is the threshold of neuron i , which is adjusted to fix the mean firing probability of neuron j to \bar{p}_j , and p_{\max} is the maximal firing probability. When $p_{\max} = 0.5$, a neuron fires, on average, only once, even if the neuron receives a sufficiently strong excitatory input twice. A small value of p_{\max} thus makes the firing of the neurons quite unreliable. Thus, p_{\max} determines the reliability with which a model neuron fires in response to an input.

To maximize information retention, our recurrent network starts from a random weight W_{ij}^{initial} and develops toward an optimized network with $W_{ij}^{\text{optimized}}$ (Fig. 1a), in a manner determined by the gradient ascent algorithm,

$$W_{ij} \leftarrow W_{ij} + \eta \frac{\partial I}{\partial W_{ij}}, \quad (2)$$

where I is the mutual information of two successive states of the network and η is the learning rate. We performed a block of simulation consisting of 10,000-50,000 time steps, updated W_{ij} at the end of the block, and then started the calculation for the next block (Fig. 1b).

We first observed the behaviour of this model network under external input. Image patches from a photograph preprocessed by a high-pass filter were used as the external input (Fig. 1c). The neurons in this network were divided into three groups. 144 on-input and 144 off-input neurons, and the 144 output neurons were randomly selected from the network (Fig. 1d1). Dots with positive

and negative values in a randomly selected 12×12 image patch excited the corresponding on-input and off-input neurons, respectively. The states of the input neurons were stochastically set to 1 or 0 with firing probabilities proportional to the intensities of the corresponding dots, whereas the states of the output neurons were not set by the external input. Instead, the firings of these neurons were determined by Eq. 1 with $p_{\max} = 0.95$. Initially, the connection weight W_{ij} was a random matrix (Fig. 1e1), and therefore the output neurons did not exhibit clear selectivity with respect to the external input from the input neurons (Fig. 1f1). After learning, however, the network self-organized a feedforward structure from the on-input and off-input neurons to the output neurons (Fig. 1e2,d2). Averaging the image patches that evoked firings in an output neuron, we found that the output neuron became highly selective to Gabor function-like stimuli (Fig. 1f2), exhibiting behaviour quite similar to the selectivity of simple cells in the V1 cortex¹⁹. Our optimization algorithm based on RI hence caused the model network to become organized into a feedforward network containing simple cell-like output neurons.

In the simulation described above, the external input was fed into the network with high response reliability ($p_{\max} = 0.95$). Next, we examined the evolution of the spontaneous activity in the neuronal network without external input. To identify repeated activity in the model network, we defined a repeated pattern as a spatial pattern of neuronal firings that occurs at least twice in a test block (Fig. 2a). Colouring repeated patterns consisting of ≥ 3 firing neurons in raster plots of the network (Fig. 2c1,c2), we found that the number of repeated patterns increased after learning. Several patterns were repeated in a sample of 250 steps as seen in Fig. 2c2, where the repeated patterns are indicated by consistently coloured circles and connected by lines. Moreover, some

patterns appeared to constitute repeated sequences. For example, sequence A, composed of the magenta, orange, and purple patterns, appears three times in Fig. 2c2. To be more quantitative, we tabulated the numbers of occurrences of repeated patterns and sequences, and compared these numbers before and after learning (Fig. 2b). We found that both repeated patterns and repeated sequences increased significantly after learning. This indicates that the present algorithm embeds not only repeated patterns but also repeated sequences of firings into the network structure as a result of the optimization. Thus, when a pattern in a sequence is activated at one step, it is highly probable that the next pattern in that sequence will be activated at the next step. This predictability means that the state of the network at one time step shares much information with the state at the next time step. Hence, we concluded that the repeated activation of an embedded sequence is an efficient way to maximize information retention in a recurrent network. These repeated patterns and sequences have been experimentally observed *in vivo*^{18,20,21} and *in vitro*^{15,16}, and their existence is suggested by the theory of cell assemblies proposed by Hebb⁸ and the theory of synfire chains proposed by Abeles⁹. We thus see that RI accounts for the appearance of cell assemblies, sequences, and synfire chains in neuronal networks.

We next examined the behaviour of the same spontaneous model in the case that the maximal firing probability was small ($p_{\max} = 0.5$). For small p_{\max} , the number of identically repeated sequences is small, and the network seems to lose structured activity. However, we found characteristic network activity consisting of firing bursts (Fig. 3a2), which are defined as consecutive firing steps that are immediately preceded and followed by “silent” steps, with no firing. We found that after learning, the distribution $P(s)$ of the burst size, s , the total number of firings in

a burst, obeys a power-law distribution $P(s) \propto s^\gamma$ with $\gamma \approx -1.5$, whereas, before learning, we have $P(s) \propto \exp(-\alpha s)$ (Fig. 3c). This result is consistent with experimental results. Beggs and Plenz¹¹ recorded the spontaneous activity of an organotypic culture from a cortex using multielectrode arrays. Defining an avalanche similarly to our burst, they found that the size distribution of avalanches is accurately fit by a power-law distribution with exponent -1.5 ¹¹. To explain this, they argued that a neuronal network is tuned to minimize the information loss and that this is realized when one firing induces an average of one firing at the next step. They showed that this condition yields the universal exponent $-3/2$, using the self-organized criticality of the sandpile model^{22,23}. This condition also holds for the present network, because each neuron with $p_{\max} = 0.5$ after learning had two strong input connections and two strong output connections on average (Fig. 3b2). The universal exponent $-3/2$ was observed in the network for small p_{\max} , but for $p_{\max} = 0.95$, the size distribution of bursts $P(s)$ in the system did not exhibit a power-law distribution, and displayed several peaks, reflecting the existence of stereotyped sequences (see Supplementary Notes). We thus conclude that RI embeds information-efficient structures in which one firing induces on average one firing at the next step in a network with small p_{\max} .

To reveal the essential mechanism responsible for the behaviour described above, we returned to the recurrent network with an external input (Fig. 4). In the learning blocks, we repeatedly stimulated neurons 1, 3, and 2 in sequence (Fig. 4a1,b1). In the successive test block, in which only neuron 1 was stimulated externally (Fig. 4a2), the firing of neuron 1 was followed by spontaneous firings of neurons 3 and 2 (Fig. 4b2, arrows), because, as we saw above, embedding a sequence of firings into the network structure is an efficient way to retain information. In addition,

the spontaneous firing of neuron 1 triggers the sequence containing the firings of neurons 3 and 2 (Fig. 4b2, double arrows). The form of the weight matrix after learning reveals that a feedforward structure starting from neuron 1 was embedded in the network (Fig. 4c). It is thus seen that RI embeds externally input temporal firing patterns into the network by producing feedforward structures, and, as a result, the network can spontaneously reproduce the patterns.

In this study we have found that RI acts to optimize the network structure by maximizing the information retained in the recurrent network. Simple cell-like activity, repeated sequences, and neuronal avalanches were realized in the model network. These characteristic types of activity resulted from the network structure embedded by the optimization algorithm. On the basis of these results, we conjecture that RI underlies the neuronal plasticity rule generating these structures and activity. We believe that RI will help us to understand the meaning of *in vivo* and *in vitro* experimental results, particularly to characterize the spontaneous activity of neurons in the context of information theory. Our next goal is to derive a plasticity rule in a bottom-up way employing RI, and to compare this rule with experimentally obtained plasticity rules.

1. Linsker, R. Self-organization in a perceptual network. *Computer* **21**, 105–117 (1988).
2. Tsukada, M., Ishii, N. & Sato, R. Temporal pattern discrimination of impulse sequences in the computer-simulated nerve cells. *Biol. Cybern.* **17**, 19–28 (1975).
3. Atick, J. J. Could information theory provide an ecological theory of sensory processing? *Network* **3**, 213–251 (1992).

4. Bell, A. J. & Sejnowski, T. J. An information-maximization approach to blind separation and blind deconvolution. *Neural Comput.* **7**, 1129–1159 (1995).
5. Olshausen, B. A. & Field, D. J. Emergence of simple-cell receptive field properties by learning a sparse code for natural images. *Nature* **381**, 607–609 (1996).
6. Bell, A. J. & Sejnowski, T. J. The ‘independent components’ of natural scenes are edge filters. *Vision Res.* **37**, 3327–3338 (1997).
7. Lewicki, M. S. Efficient coding of natural sounds. *Nat. Neurosci.* **5**, 356–363 (2002).
8. Hebb, D. O. *The Organization of Behavior; a Neuropsychological Theory* (Wiley, New York, 1949).
9. Abeles, M. *Corticonics* (Cambridge Univ. Press, Cambridge, 1991).
10. Diesmann, M., Gewaltig, M. O. & Aertsen, A. Stable propagation of synchronous spiking in cortical neural networks. *Nature* **402**, 529–533 (1999).
11. Beggs, J. M. & Plenz, D. Neuronal avalanches in neocortical circuits. *J. Neurosci.* **23**, 11167–11177 (2003).
12. Teramae, J.-N. & Fukai, T. Local cortical circuit model inferred from power-law distributed neuronal avalanches. *J. Comput. Neurosci.* **22**, 301–312 (2007).
13. Abbott, L. & Rohrkeper, R. A simple growth model constructs critical avalanche networks. *Prog. Brain Res.* **165**, 13–19 (2007).

14. Nadasdy, Z., Hirase, H., Czurko, A., Csicsvari, J. & Buzsaki, G. Replay and time compression of recurring spike sequences in the hippocampus. *J. Neurosci.* **19**, 9497–9507 (1999).
15. Cossart, R., Aronov, D. & Yuste, R. Attractor dynamics of network UP states in the neocortex. *Nature* **423**, 283–288 (2003).
16. Ikegaya, Y. *et al.* Synfire chains and cortical songs: temporal modules of cortical activity. *Science* **304**, 559–564 (2004).
17. Fujisawa, S., Matsuki, N. & Ikegaya, Y. Single neurons can induce phase transitions of cortical recurrent networks with multiple internal States. *Cereb. Cortex* **16**, 639–654 (2006).
18. Sakurai, Y. & Takahashi, S. Dynamic synchrony of firing in the monkey prefrontal cortex during working-memory tasks. *J. Neurosci.* **26**, 10141–10153 (2006).
19. Hubel, D. H. & Wiesel, T. N. Receptive fields of single neurones in the cat's striate cortex. *J. Physiol.* **148**, 574–591 (1959).
20. Skaggs, W. E. & McNaughton, B. L. Replay of neuronal firing sequences in rat hippocampus during sleep following spatial experience. *Science* **271**, 1870–1873 (1996).
21. Yao, H., Shi, L., Han, F., Gao, H. & Dan, Y. Rapid learning in cortical coding of visual scenes. *Nat. Neurosci.* **10**, 772–778 (2007).
22. Bak, P., Tang, C. & Wiesenfeld, K. Self-organized criticality: An explanation of the 1/f noise. *Phys. Rev. Lett.* **59**, 381–384 (1987).
23. Harris, T. E. *The theory of branching processes* (Dover, New York, 1989).

Acknowledgements This work was supported by Grants-in-Aid from the Ministry of Education, Science, Sports, and Culture of Japan: Grant numbers 16200025, 17022020, 17650100, 18019019, 18047014, and 18300079.

Author Information The authors declare that they have no competing financial interests. Correspondence and requests for materials should be addressed to ttakuma@mbs.med.kyoto-u.ac.jp.

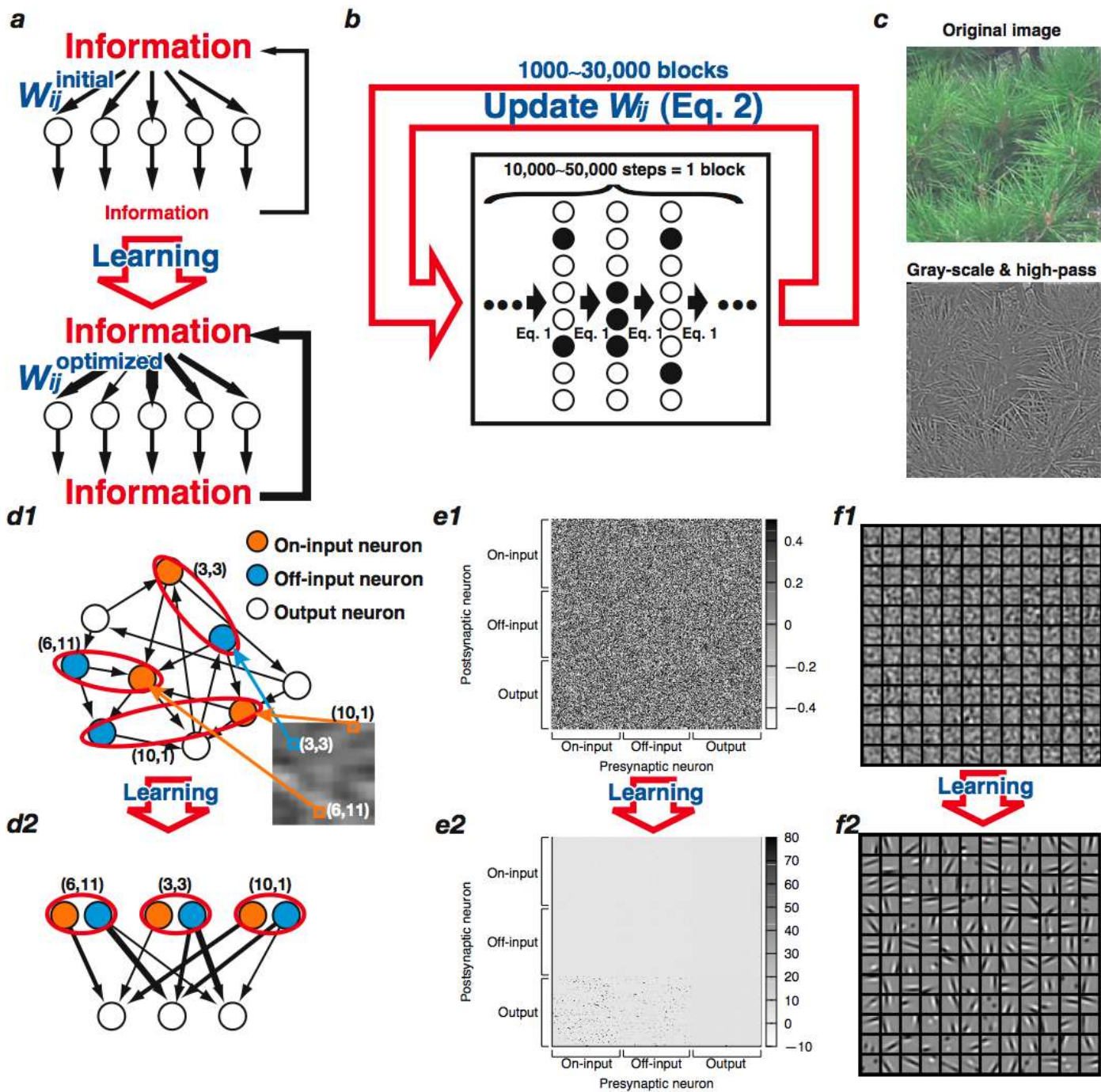


Figure 1

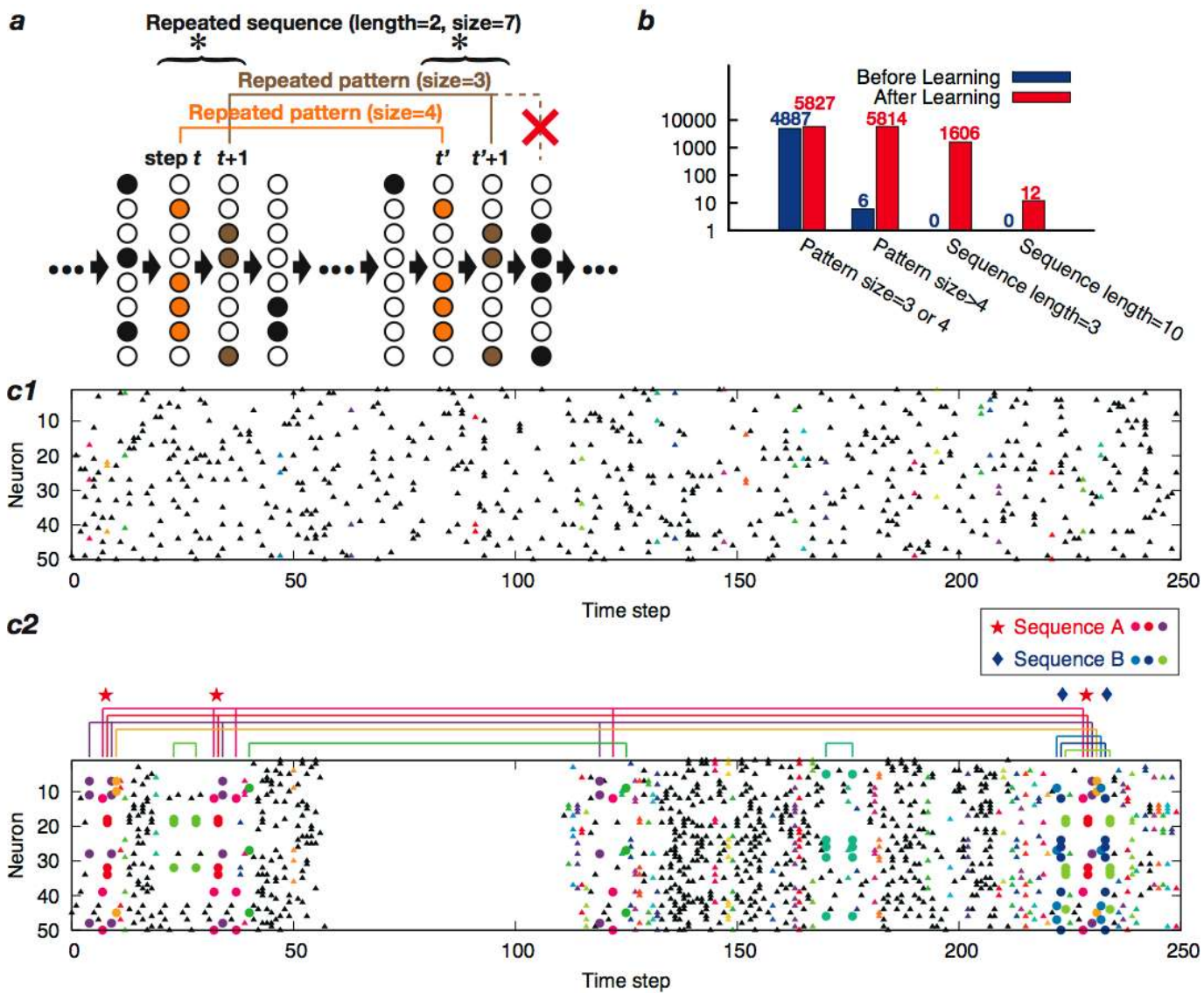


Figure 2

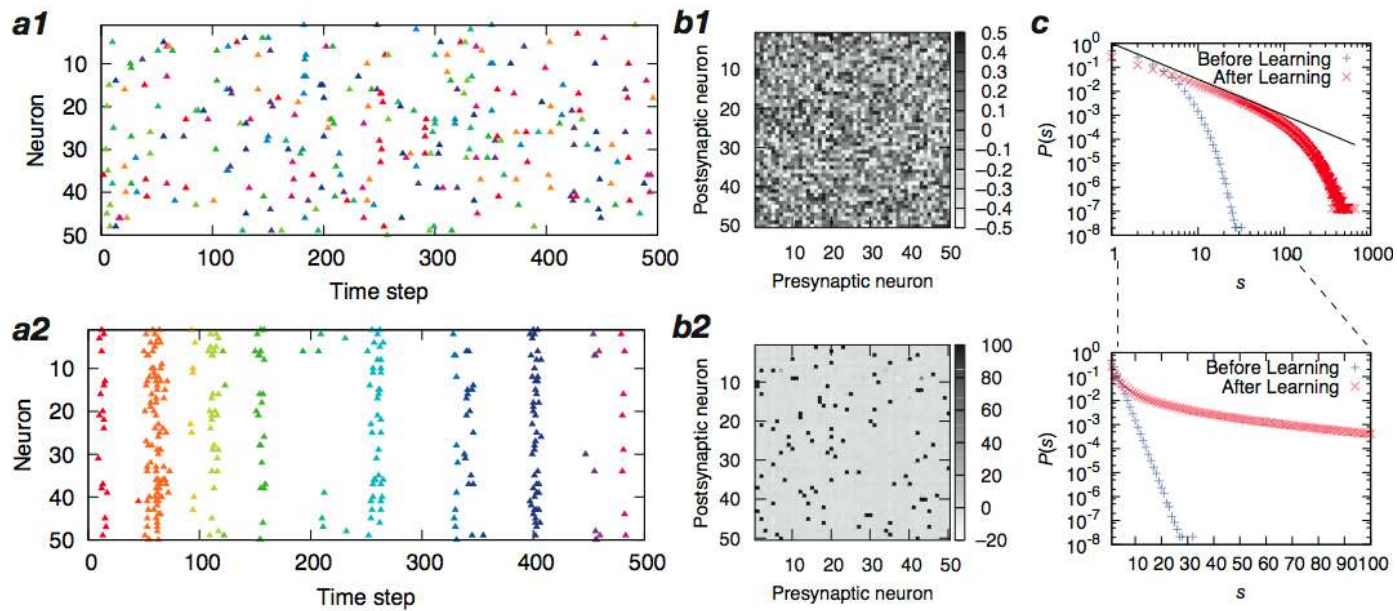


Figure 3

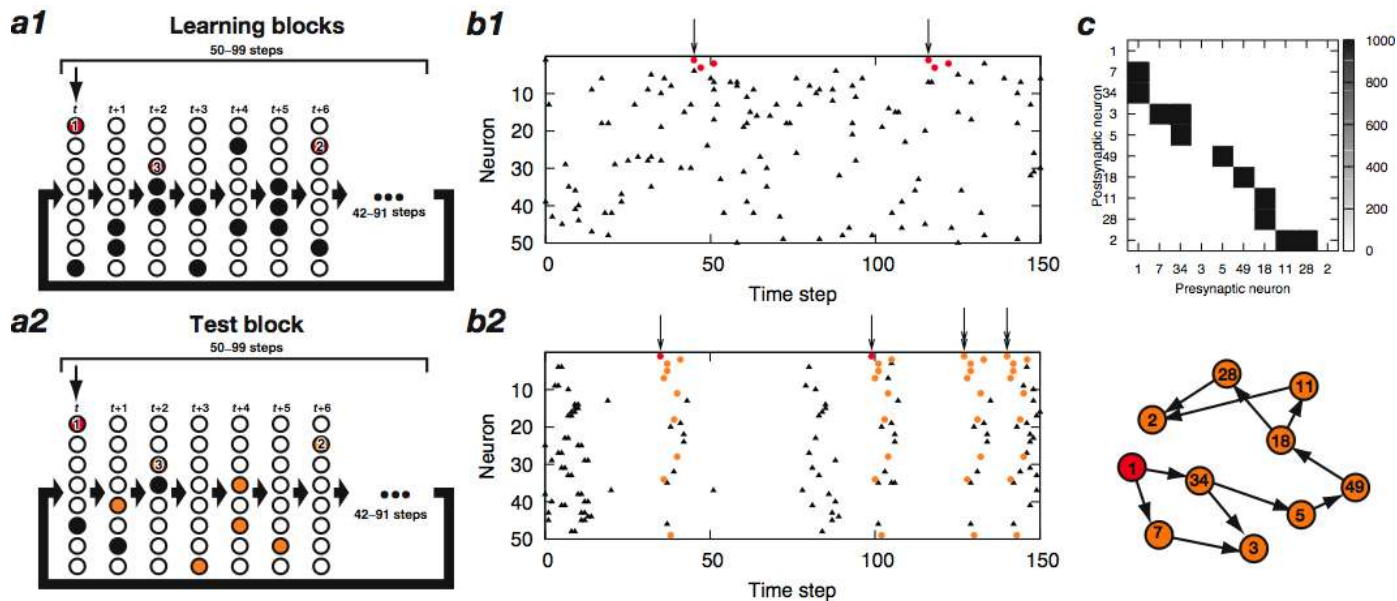


Figure 4

Figure 1 Formation of the feedforward structure through an algorithm based on RI in the model network with external input. (a) Learning changes the initial weight matrix W_{ij}^{initial} to $W_{ij}^{\text{optimized}}$ so as to maximize the information retained in a recurrent network. (b) In the simulation, W_{ij} was updated using Eq. 2 at the end of each block, which consists of 10,000-50,000 steps. (c) The original photograph (1024×1024) of a pine tree was converted to a gray-scaled, high-pass filtered image. Image patches (12×12) randomly selected from the high-pass filtered image were used as the external inputs to the network at each time step. (d1,e1) Initially, 432 neurons were connected according to a random weight matrix. Of these neurons 144 were on-input, 144 were off-input, and 144 were output neurons. Each of the 144 dots in an image patch was linked to a pair of an on- and an off-input neuron in such a manner that the on-input and off-input neurons were set to 1 (fire) only when the corresponding dot had a positive and negative sign, respectively. Output neurons fired spontaneously according to Eq. 1. (d2,e2) After learning, feedforward structure from input to output neurons appeared in the model network. (f1,2) Averaging the image patches that evoked firings of the output neurons revealed that the output neurons, which did not exhibit clear selectivity before learning, responded to the Gabor-like stimulus after learning.

Figure 2 Repeated spatial patterns and spatiotemporal sequences occurred frequently in the network with $p_{\text{max}} = 0.95$ after learning. (a) We define a repeated pattern as a spatial firing pattern that is identically repeated at different time steps. The size of a pattern is defined as the number of neurons firing in the pattern. A sequence that contains

a particular set of patterns appearing repeatedly in the same temporal order is called a “repeated sequence.” The size of a repeated sequence is defined as the sum of the sizes of the patterns contained in it. (b) The numbers of occurrences of the patterns and sequences repeated in the test block (50,000 steps) were compared before and after learning. In this histogram, only the sequences with sizes larger than $5l$, where l is the length of the sequence, were counted. (c1,2) When the repeated patterns in the 50,000 steps were coloured, it was found that no pattern occurred more than once in this short raster plot before learning (c1). By contrast, several patterns appeared multiple times in the raster plot after learning (c2). In addition, repeated sequences were found only in the raster plot after learning (red stars and blue diamonds).

Figure 3 Spontaneous activity of the recurrent network with $p_{\max} = 0.5$. (a1,2) Individual bursts in the spontaneous activity before (a1) and after learning (a2) are indicated by different colours. The bursts before learning were short and frequently interrupted by steps without firing, whereas the bursts after learning had much longer durations. (b1,2) The initial W_{ij} with random weights evolved into a matrix with relatively few strong weights. Most rows and columns contained two strong excitatory connections (black dots); that is, most neurons had two strong inputs and two strong outputs. (c) Frequency distribution $P(s)$ of the burst size plotted as a function of the size, s . The black line corresponds to a slope of -1.5 .

Figure 4 A feedforward structure was embedded in the model network by the temporally-structured stimulation. (a1,2) In the learning blocks, the state of neuron 1 was set to 1 (fire) at random intervals ranging from 50 to 99 steps. The first time step, t , is indicated by the arrow in a1. At $t + 2$, the state of neuron 3 was set to 1, and at $t + 6$, the state of neuron 2 was set to 1. In the test block after learning, only neuron 1 was set to 1 at random intervals ranging from 50 to 99 steps (a2). External stimulations are indicated by red circles. (b1, 2) The network activity in an early learning block (b1) and the test block (b2). The steps at which neuron 1 was set to 1 are indicated by arrows, and externally evoked firings of neurons 1, 2, and 3 are indicated by red circles. Although the states of neurons 2 and 3 were not set from the outside during the test block, neurons 2 and 3 fired spontaneously six and two steps, respectively, after neuron 1 fired (as indicated by orange circles). The sequence of firings embedded by learning was replayed after the spontaneous firing of neuron 1 (double arrows). (c) The weight matrix of the network after learning (top) and its schematic representation (bottom) indicate a feedforward structure which underlies the firing sequence starting from neuron 1 and containing neurons 3 and 2.